# ANNEXURE A

Unit for Drug Research and Development, Faculty of Health Sciences, North-West University, Potchefstroom, South Africa

# A novel reversed-phase LC method for quantitative detection of azithromycin in bulk drug and tablet formulations in various aqueous media

R. W. Odendaal, W. Liebenberg, M. E Aucamp

*Received February 17, 2012, accepted April 5, 2012*

*M.E. Aucamp, Internal box 36, Private bag X6001, Potchefstroom Campus, North-West University, Potchefstroom 2520, South Africa*
*Marique.Aucamp@nwu.ac.za*

*Pharmazie 67: 1–3 (2012)* *doi: 10.1691/ph.2012.2041*

A novel reversed-phase HPLC method with UV-detection for separation, identification and quantification of azithromycin (AZH) was developed. The method was validated for the purpose of quantifying AZH in stability, dissolution and solubility studies. The method was validated at two optimum wavelengths where linear regression at both 205 and 210 nm, resulted in correlation coefficients of $r^2 = 0.9999$. This HPLC method proved to be superior to other published methods due to the specificity, resulting in less peak interference and tailing. The pH of the mobile phase, as well as the ratio of buffer to organic component included in the mobile phase, proved to be critical factors in the improved detection of AZH.

## 1. Introduction

Azithromycin (AZH), a semi-synthetic macrolide, is considered to be one of the world's best-selling antibiotics (Miroshnyk et al. 2006). Previously published HPLC methods for the identification and/or quantification of AZH include electrochemical or UV detection (Kanfer et al. 1998; Miguel and Barbas 2003; Shaikh et al. 2008). Methods using electrochemical (coulometric and amperometric) detection for AZH in biological samples have been reported by Shepard et al. (1991). The USP describes an assay, using an amperometric method for detection (USP 2010). Zubata et al. (2002) described an HPLC method using UV-detection to identify AZH and its impurities present in AZH tablets. These methods utilize equipment not readily available in many laboratories. In this study, an HPLC method with UV-detection was developed. Poor UV absorbance imposes the problem of limited detection of AZH (Kanfer et al. 1998), but the specificity and clear separation of this novel method compensate for and overcome this limitation. Known published HPLC methods (Kanfer et al. 1998; Miguel and Barbas 2003; Shaikh et al. 2008; Shepard et al. 1991; USP 2010; Zubata et al. 2002) for the quantification of AZH were investigated, and all methods used had different constituents for the mobile phase at variable pH, ranging from 3 to 9. The aim of this paper was to develop and validate a reliable HPLC method to identify and/or quantify AZH during product assays, solubility, stability, and dissolution studies.

## 2. Investigations, results and discussion

During the method development stage it became clear that pH and composition of the mobile phase were critical factors. For a mobile phase with pH < 6 the AZH peak overlapped significantly with mobile phase peaks and poor peak separation was prevalent. This mobile phase also resulted in a very short retention time for the AZH peak. This posed to be problematic, especially for the detection of AZH in solubility and/or dissolution media. The interference of the aqueous media caused very poor peak identification, separation and unreliable peak area integration. For pH > 6 the symmetry of the AZH peak was poor. The absence of symmetrical peaks was due to peak tailing which made peak area integration inaccurate and quantitative repeatability impossible.

Method validation of the developed method was established at two wavelengths, 205 and 210 nm. The proposed method was validated for linearity, range, precision, accuracy, recovery, specificity, robustness, limit of detection (DL) and limit of quantitation (QL). Five calibration standard solutions with concentrations ranging from 0.1 mg/mL to 5.0 mg/mL, were prepared. Accuracy was determined by injecting duplicate injections of the calibration control solutions (100% theoretical concentration). The recovered concentration was compared to the initial theoretical concentration of the control solutions (Table). To determine specificity, a commercial AZH tablet was dissolved in mobile phase. Specificity was also resolved by dissolving AZH at a known concentration in the four general solubility media (acetate and phosphate buffer, 0.1 M HCl and water). Precision of this method was assessed on two levels: repeatability and intermediate precision (robustness). Repeatability was measured through repeated injections (5 replicates) of the calibration standard solutions that represent 100% theoretical concentration. Data recovered from the five replicate injections of the 100 % solution (1.0 mg/mL), at both wavelengths, showed RSD values of 0.16 % and 0.17 % respectively. To establish robustness, this method was performed by two different analysts in the same laboratory on consecutive days. The chromatographic columns and the HPLC systems used were different. The results obtained during the robustness testing proved that this method is accurate in retaining AZH without peak interference. At wavelength 205 nm the equation

**Table: Results obtained during the method validation**

| Wavelength (nm) | Range (μg.ml$^{-1}$) | *$R^2$ | Accuracy (%) | RSD (%) | *DL (μg/ml) | *QL (μg/ml) |
|---|---|---|---|---|---|---|
| 205 | 100.0–5000.0 | 0.9999 | 100.68 ± 0.06 | 0.06 | 3.88 | 11.76 |
| 210 | 100.0–5000.0 | 0.9999 | 100.74 ± 0.06 | 0.06 | 6.87 | 20.80 |

*$R^2$ - Correlation coefficient
*DL - Limit of detection
*QL - Limit of quantitation
*The calculated P-values at a confidence level of 95% for the curves obtained at 205 nm and 210 nm were 0.293 and 0.424 respectively*

for regression (y = 218.03x + 4213.21) had a correlation coefficient of 0.9983, with percentage recovery (%) of 104.95% (RSD = 0.3%). At wavelength 210 nm the equation for regression (y = 139.89x + 3948.10) had a correlation coefficient of 0.9970, with a recovery of 106.66% (RSD = 0.3%).

During the test for specificity the inactive ingredients included in the commercial AZH tablet did not show any interference, at both wavelengths, towards the AZH peak. Peaks, due to tablet excipients, were detected at retention times of approximately 8.0 and 14.0 min (Fig.). The solution of the commercial AZH tablet was also spiked with azithromycin in order to confirm that the unknown peaks at 8.0 and 14.0 min are not due to azithromycin. A blank mobile phase sample was injected to conclude the presence, but not interference, of small peaks due to the buffer and solvents used in the mobile phase. From the Fig. it is clear that these unknown substances (tablet excipients) cause no interference with the chromatography.

Blank samples containing only solubility media were initially injected to identify peaks due to the buffer contents in each medium. The prepared samples with an AZH concentration of 1.0 mg/mL were injected after the blank samples. Chromatograms (Fig. c–f) revealed the clear separation of the AZH peak from the other peaks (solubility media peaks). A blank water sample was also injected, followed by a sample of AZH dissolved in water (0.1 mg/mL). With previously developed methods, the use of water as solvent made integration and quantification of AZH difficult. With this method there is sufficient separation to integrate the AZH peak for quantification. The peaks that represent water on the chromatogram did not cause any interference with the AZH peak (Fig. c). Despite the poor water solubility of AZH in water and the difficulty it causes to quantify very low concentrations of this API in water, this method still produced clear separation and an AZH peak that can be accurately quantified. Data recovered from the five replicate injections of the 100% solution (1.0 mg/mL), at both wavelengths, showed RSD values of 0.16% and 0.17% respectively. The smallest concentration of analyte in a sample that the method is able to detect, but not essentially quantified, can be described as the limit of detection (DL) (USP 2010). The quantitation limit (QL) can be expressed as the smallest analyte concentration in a sample which the method is capable of quantifying with apt accuracy and precision (USP 2010). An Excel™ spreadsheet (Analysis ToolPak) using linear regression was utilized to calculate the DL and QL.

A novel reversed phase HPLC method using UV-detection has been developed as a multi-purpose method to identify and quantify AZH in drug samples. This method showed to be sensitive but also robust enough so that it can successfully be exploited during stability, solubility and dissolution studies of AZH. From the data obtained during method development, it became clear that the pH of the mobile phase used, and ratio of buffer to organic component, is critical for the optimum detection of AZH.

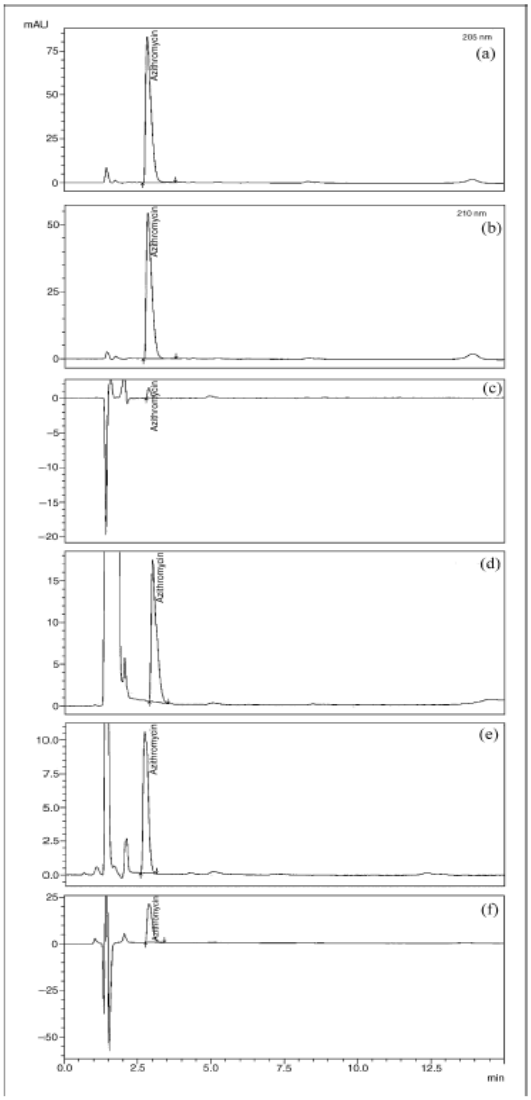


Fig.: A typical chromatogram of azithromycin tablet (5 mg/mL), dissolved in mobile phase, at (a) 205 nm and (b) 210 nm. Mobile phase: phosphate buffer (adjusted with 1.0 M sodium hydroxide to pH 6.0)/acetonitrile (700:300), flow rate 1.0 mL/min, injection volume 15 μL. Column: reversed phase C18, 5 μm, 150 mm x 4.6 mm. UV-detection: 205 nm and 210 nm and chromatograms obtained for azithromycin dissolved in (c) distilled water (0.1 mg/ml), (d) acetate buffer pH 4.5 (1.0 mg/ml), (e) phosphate buffer pH 6.8 (0.5 mg/ml) and (f) 0.1 M HCl (1.0 mg/ml)

## 3. Experimental

AZH with a purity of 96.5% (on dried basis) was purchased from DB Fine Chemicals (Batch number: IF-AZ080506). A Shimadzu (Kyoto Japan) UFLC (LC-20AD) chromatographic system was utilized. The system consisted of a SIL-20AC auto-sampler fitted with a sampler cooler, a UV/VIS Photodiode Array detector (SPD-M20A) and a LC-20AD solvent delivery module. A Phenomenex® Luna C18 (5 μm) 150 mm × 4.6 mm column was

used as stationary phase. The mobile phase consisted of a combination of 0.06 M phosphate buffer at pH 6.0 (pH adjusted with 1.0 M NaOH), and acetonitrile (700:300). Isocratic elution was used. The flow rate was set at 1.0 mL/min. Photodiode array detection showed that two wavelengths, namely 205 and 210 nm, were most favourable for detection. Injection volume for each sample was 15 µL. The four media utilized to determine the application of this method for solubility and dissolution studies are phosphate buffer (pH 6.8), acetate buffer (pH 4.5), 0.1 M HCl (pH 1.2), and water (BP 2011).

## References


Amsden GW (2001) Advanced-generation macrolides: Tissue-directed antibiotics. Int J Antimicrob Agents 18: 11–15.

Amsden GW (1996) Erythromycin, clarithromycin, and azithromycin: Are the differences real? Clin Ther 18: 56–72.

BP 2011 Volume V. Appendix A: A67, A100, A147.

Hoepleman IM, Scneider MME (1995) Azithromycin: The first of the tissue-selective azalides. Int J Antimicrob Agents 5: 145–167.

Kanfer I, Skinner MF, Walker RB (1998) Analysis of macrolide antibiotics. J Chromatogr A 812: 255–286.

Kremer CJ (2002) Azithromycin—a new macrolide. *Primary care update for Ob/Gyns*, 9: 174–175.

Miguel L, Barbas C (2003) LC determination of impurities in azithromycin tablets. J Pharm Biomed Anal 33: 211–217.

Miroshnyk I, Mirza S, Zorky PM, Heinämäki J, Yli-Kauhaluoma J, Yliruusi J (2008) A new insight into solid-state conformation of macrolide antibiotics. Bioorg Med Chem 16: 232–239.

Shah RD, Maryanoff CA (2001) Reversed phase HPLC.(*In* J.K. Swadesh *ed., HPLC: practical and industrial applications*. Florida: CRC Press, p. 153).

Shaikh KA, Patil SD, Devkhile AB (2008) Development and validation of a reversed-phase HPLC method for simultaneous estimation of ambroxol hydrochloride and azithromycin in tablet dosage form. J Pharm Biomed Anal 48: 1481–1484.

Shepard RM, Duthu GS, Ferraina RA, Mullins MA (1991) High-performance liquid chromatography assay with electrochemical detection for azithromycin in serum and tissues. J Chromatogr 565: 321–337.

USP 33, National Formulary 28, re-issue. The United States Pharmacopeial Convention, 2010 NF28 edition (2010).

Yang ZY, Wang L, Tang X (2009) Determination of azithromycin by ion-pair HPLC with UV detection. J Pharm Biomed Anal 49: 811–815.

Zubata P, Ceresole R, Rosasco MA, Pizzorno MT (2002) A new HPLC method for azithromycin quantitation. J Pharm Biomed Anal 27: 833–836.

# ANNEXURE B

(12) INTERNATIONAL APPLICATION PUBLISHED UNDER THE PATENT COOPERATION TREATY (PCT)

(19) World Intellectual Property Organization
International Bureau

(43) International Publication Date
23 June 2011 (23.06.2011)

PCT

(10) International Publication Number
WO 2011/073927 A1

(51) International Patent Classification:
*C07H 17/08* (2006.01) *C07H 1/00* (2006.01)

(21) International Application Number:
PCT/IB2010/055842

(22) International Filing Date:
15 December 2010 (15.12.2010)

(25) Filing Language: English

(26) Publication Language: English

(30) Priority Data:
2009/09098 18 December 2009 (18.12.2009) ZA

(71) Applicant *(for all designated States except US)*: **NORTH-WEST UNIVERSITY** [ZA/ZA]; 1 Hoffman Street, Joon van Rooy Building, 2531 Potchefstroom (ZA).

(72) Inventors; and

(75) Inventors/Applicants *(for US only)*: **ODENDAAL, Roelf, Willem** [ZA/ZA]; Quantum Estate, Oudedorp, 2531 Potchefstroom (ZA). **LIEBENBERG, Wilna** [ZA/ZA]; 2 Kiewiet Street, Baillie Park, 2531 Potchefstroom (ZA). **AUCAMP, Marique** [ZA/ZA]; 2 Scheepers Street, 2531 Potchefstroom (ZA).

(74) Agent: **DM KISCH INC.**; P O Box 781218, 2146 Sandton (ZA).

(81) Designated States *(unless otherwise indicated, for every kind of national protection available)*: AE, AG, AL, AM, AO, AT, AU, AZ, BA, BB, BG, BH, BR, BW, BY, BZ, CA, CH, CL, CN, CO, CR, CU, CZ, DE, DK, DM, DO, DZ, EC, EE, EG, ES, FI, GB, GD, GE, GH, GM, GT, HN, HR, HU, ID, IL, IN, IS, JP, KE, KG, KM, KN, KP, KR, KZ, LA, LC, LK, LR, LS, LT, LU, LY, MA, MD, ME, MG, MK, MN, MW, MX, MY, MZ, NA, NG, NI, NO, NZ, OM, PE, PG, PH, PL, PT, RO, RS, RU, SC, SD, SE, SG, SK, SL, SM, ST, SV, SY, TH, TJ, TM, TN, TR, TT, TZ, UA, UG, US, UZ, VC, VN, ZA, ZM, ZW.

(84) Designated States *(unless otherwise indicated, for every kind of regional protection available)*: ARIPO (BW, GH, GM, KE, LR, LS, MW, MZ, NA, SD, SL, SZ, TZ, UG, ZM, ZW), Eurasian (AM, AZ, BY, KG, KZ, MD, RU, TJ, TM), European (AL, AT, BE, BG, CH, CY, CZ, DE, DK, EE, ES, FI, FR, GB, GR, HR, HU, IE, IS, IT, LT, LU, LV, MC, MK, MT, NL, NO, PL, PT, RO, RS, SE, SI, SK, SM, TR), OAPI (BF, BJ, CF, CG, CI, CM, GA, GN, GQ, GW, ML, MR, NE, SN, TD, TG).

**Published**:

— *with international search report (Art. 21(3))*

WO 2011/073927 A1

(54) **Title**: COMPOSITION COMPRISING AN AMORPHOUS NON- CRYSTALLINE GLASS FORM OF AZITHROMYCIN

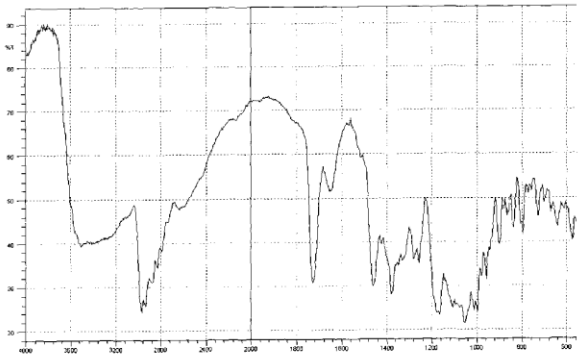

FIGURE 2

(57) **Abstract**: The invention relates to an amorphous non-crystalline glass form (2R,3S,4R,5R,8R,10R,11R,12S,13S,14R) -2-ethyl-3,4, 10- trihydroxy- 3,5,6,8,10,12,14- heptamethyl-15-oxo- 11- {[3,4,6- trideoxy-3- (dimethylamino) -β-D-xylo- hexopyranosyl]oxy}-1-oxa- 6- azacyclopentadec-13-yl 2,6-dideoxy-3-C-methyl-3-O-methyl-α-L-ribo- hexopyranoside or azithromycin having an infra-red pattern displaying characteristic relatively broad peaks at approximately 3500 and 1727 $cm^{-1}$ and characteristic peaks at approximately 2970 and 2938 $cm^{-1}$. The invention further relates to a preparation method of increasing the solubility of azithromycin including the steps of selecting anhydrous, monohydrated or dihydrated azithromycin; elevating the temperature of the azithromycin to above the melting point thereof; and reducing the temperature of the melt sufficiently to allow it to set into an amorphous non-crystalline glass form (Form-II) of azithromycin having relatively increased solubility without decreasing the structural stability thereof.

# ANNEXURE C

**An amorphous azithromycin form with improved water solubility and membrane permeability**

Marique Aucamp[a], Roelf Odendaal[a], Wilna Liebenberg[a], Sias Hamman[a,*]

[a]Center of Excellence for Pharmaceutical Sciences, North-West University, Private Bag X6001, Potchefstroom, 2520, South Africa.

*Corresponding author:

Hamman JH (PhD)

Research Professor

Center of Excellence for Pharmaceutical Sciences,

North-West University,

Private Bag X6001,

Potchefstroom,

2520,

South Africa

E-mail: sias.hamman@nwu.ac.za

Tel: +27 18 299 4035,

Fax: +27 18 2935219

**Abstract**

Azithromycin is a poorly soluble macrolide antibacterial agent. This is seen as the major contributing factor to its relatively low oral bioavailability. The aim of this study was to improve the solubility of this API by preparing an amorphous form by quench cooling of the melt. Comparison of the physico-chemical properties of both crystalline and amorphous azithromycin was done through DSC, TGA, FTIR, XRPD, Vapor sorption, equilibrium solubility as well as dissolution studies. The amorphous azithromycin exhibited a significant increase in water solubility when compared to the crystalline azithromycin dihydrate. The influence that the improved solubility could have on permeability was also studied. The apparent permeability coefficient ($P_{app}$) values of amorphous azithromycin were statistically significantly higher ($p < 0.05$) than crystalline azithromycin dihydrate at pH values of 6.8 and 7.2, while it was lower at pH 4.5. The results therefore indicated that the improved solubility of azithromycin in the amorphous form also produced improved permeability across excised intestinal tissue at physiological pH values found in the small intestine.

**Key words:** Azithromycin, amorphous, apparent permeability coefficient, *in vitro* permeability,

## Introduction

Azithromycin (AZM) is a semisynthetic macrolide antibiotic, being derived from erythromycin, resulting in a 15-membered lactone ring (Figure 1) and is classified as the first member of the azalide class of antibiotics. AZM differs from erythromycin by the insertion of a methyl-substituted nitrogen atom within the ring (1-5). AZM acts as a bacteriostatic or bactericidal agent through the inhibition of RNA-dependent bacterial protein synthesis and proves to be effective against gram-negative or gram-positive microorganisms (3). Literature reports AZM to exist in at least three crystalline forms, namely; anhydrous, monohydrate and dihydrate. A major disadvantage of AZM is the fact that it is very poorly soluble in aqueous environments (≅ 0.1 $mg.mL^{-1}$), which contributes to its relatively low absolute oral bioavailability of only 37% (3,6).

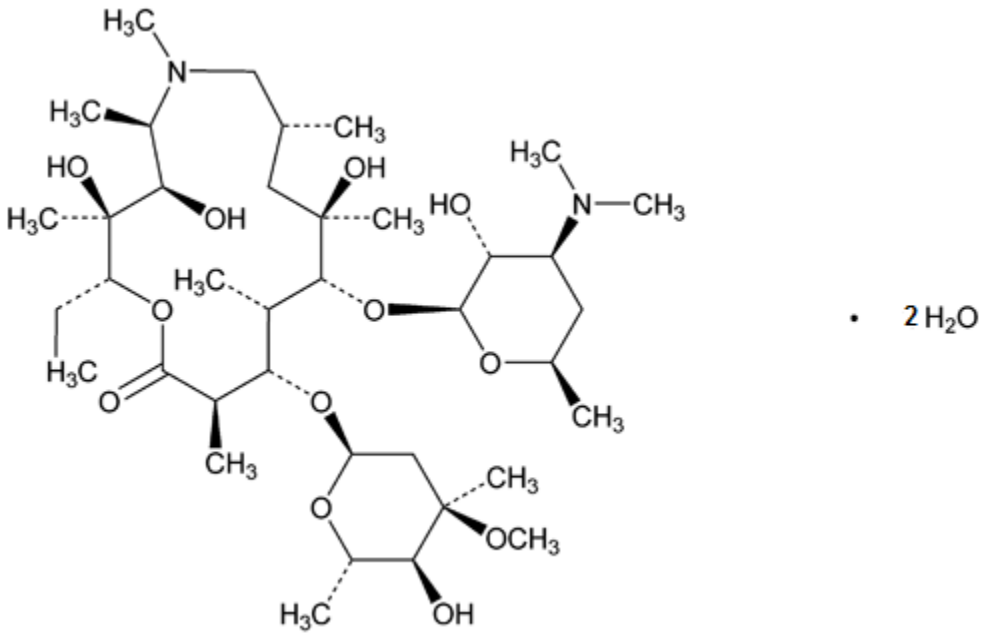


**Figure 1:** Molecular structure of azithromycin dihydrate (5).

Poor water solubility could lead to variable dissolution rates and ultimately such a drawback will detrimentally influence the bioavailability and subsequent treatment of patients. The

improvement of the dissolution and solubility properties of such APIs remains a challenging task within the pharmaceutical industry. Several methods can be employed to improve the aqueous solubility of an API. These methods include the formulation of solid dispersions, particle size reduction, complexation, use of hydrophilic carriers in order to improve wettability or preparation of the amorphous form of a given API. In comparison with the crystalline state of APIs, the amorphous state show higher dissolution rates and increased apparent solubility due to the higher degree of free energy. However, the stability usually decreases with an increase in free energy. Amorphous solids therefore tend to be thermodynamically unstable in comparison with their crystalline equivalents (7).

The rate as well as the extent of drug transported across a biological membrane can be collectively described as the permeability of the drug. *In vitro* permeation of a drug across epithelial cell membranes can be used to establish an estimation of its oral absorption within the human body. *In vitro* methods for investigating intestinal drug absorption include determining the partition coefficient (log P) value, transport across artificial membranes, transport across cultured cell monolayers, transport across excised tissue sheets and surface plasmon resonance biosensor analysis (8). The most commonly used *ex vivo* techniques for drug transport studies include excised sheets of intestinal mucosa mounted in Ussing type chambers (9) and everted intestinal rings or closed everted sacs (10). These *in vitro* permeability assays are effective and insightful in the early screening of the pharmacokinetic properties of new and improved drug compounds (11-13). Excised pig intestinal tissue has been shown to be a feasible *in vitro* model to measure drug transport with only mild signs of tissue deterioration after 120 minutes incubation time (14).

In this study we report on the preparation of an amorphous form of azithromycin (AZM-A), as well as the evaluation of the physico-chemical and membrane permeability properties of

amorphous azithromycin (AZM-A) compared to that of crystalline azithromycin dihydrate (AZM-DH).

## Materials and methods

### Materials

Azithromycin dihydrate (AZM-DH) raw material was purchased from DB Fine Chemicals (Pty) Ltd (Johannesburg, South Africa). This crystalline form of azithromycin was used to prepare amorphous azithromycin (AZM-A). Krebs Ringer bicarbonate buffer and sodium bicarbonate was purchased from Sigma Aldrich (Johannesburg, South Africa). All other reagents were either of chromatography or analytical grade. The pig intestinal tissue was obtained from freshly slaughtered pigs at Potchefstroom abattoir (Potchefstroom, South Africa) and the transport study on excised pig intestinal tissue was approved by North-West University ethics committee (NWU-0018-09-A5).

### Preparation and characterisation of different azithromycin forms

### Preparation of amorphous azithromycin

Azithromycin dihydrate (AZM-DH) was used to prepare amorphous azithromycin (AZM-A) by heating it in an oven (Binder GmbH, Germany) with the temperature set to 130°C ± 5°C. The AZM-DH was allowed to melt completely, followed by quench cooling of the molten mass to room temperature. The purity of azithromycin was determined by HPLC analysis after the preparation in order to confirm that no degradation occurred during the heating process. The amorphous habit was confirmed by XRPD.

**Fourier Transform Infrared Spectroscopy (FTIR)**

A Shimadzu IR Prestige-21 spectrometer (Kyoto, Japan) was used to record infrared (IR) spectra. The spectra were recorded over the range of 400 - 4000 $cm^{-1}$. Potassium bromide was used as a background. The sample was dispersed in a matrix of powdered potassium bromide and through diffuse reflectance infrared Fourier transform spectroscopy, IR-spectra was measured in a reflectance cell.

**X-ray powder diffraction (XRPD)**

The X-Ray powder diffraction was done using a Phillips X'Pert Pro diffractometer (PANalytical, Almelo, Netherlands). The measurement conditions for all scans were set as follows: target, Cu; voltage, 40 kV; current, 40 mA; divergence slit, 2 mm; anti-scatter slit, 0.6 mm; detector slit, 0.2 mm; scanning speed, 2°/min (step size, 0.025°; step time, 1.0 sec).

**Scanning electron microscopy (SEM)**

SEM images of AZM-DH and AZM-A were used to identify any morphological differences. The samples were prepared by fixing it to a small piece of carbon tape, mounted on a metal stub and coated with gold/palladium using an Eiko Engineering ion coater IB-2 (Eiko Engineering, Ibaraki, Japan). The samples were then imaged using a field-emission SEM, Quanta 200 ESEM (FEI Corporation, Hillsboro, USA).

**Differential scanning calorimetry (DSC)**

A Shimadzu DSC-60 instrument (Kyoto, Japan) was used to record the DSC thermograms. Approximately 3 – 5 mg of sample was accurately weighed and sealed in aluminium crimp cells with pierced lids. The samples were heated from 25 - 150°C with a heating rate of 2°C/min and a nitrogen gas purge of 35 mL/min. The onset temperatures of the thermal events are reported.

**Thermogravimetric analysis (TGA)**

A Shimadzu TGA-60 instrument (Kyoto, Japan) was used to determine the percentage weight loss (%) of AZM-DH and AZM-A. Approximately 3 – 5 mg of the sample was accurately weighed into open aluminium sample crucibles. The samples were heated from 25°C to 150ºC with a heating rate of 2°C/min, with a nitrogen gas purge of 35 mL/min.

**Karl Fischer titration**

Karl Fischer titrations were performed on samples to determine the total moisture content. The instrument used was a Metrohm 870 KF Titrino Plus autotitrator (Herisau, Switzerland). It was calibrated using a predetermined mass of water (25 - 30 µl) and a Hydranal® water standard 10.0 [1 g (1 ml at 20°C) containing 10.0 mg = 1 % water]. Approximately 100 mg of each sample was used for the moisture determination. The titration experiment was performed in triplicate for each sample.

**Vapor sorption analysis**

The moisture sorption analyses were performed utilizing a VTI-SA vapor sorption analyzer (TA Instruments, USA). The microbalance was calibrated prior to each vapor sorption run with a 100 mg standard weight. The microbalance was set to zero prior to weighing of the sample into the stainless steel sample container. The sample was carefully placed into the sample holder and care was taken to evenly distribute the sample. The percentage relative humidity (% RH) / temperature program was set using TA Instruments Isotherm software. The % RH ramp was set from 5 - 95% RH, followed by a decrease in % RH from 95 - 5%. A drying phase of 40°C with a weight loss criterion of not more than 0.01% weight loss in 2 minutes was set to run prior the % RH ramp program. The temperature was set at a constant 25°C throughout the % RH ramp. The program criteria were set to 0.0001% weight change or 2-minute stability of weight gained or lost before the program would continue to the next set parameter.

**Equilibrium solubility in different media**

The solubility of the two AZM forms was determined in deionised water as well as in various buffered media (at pH 4.5; 6.8 and 7.2) used for the permeability study. AZM-DH and AZM-A powders were individually weighed (200 mg) and placed in 20 mL amber glass tubes with screw-caps after which 10 mL of the appropriate medium was added to each glass tube to produce an over-saturated solution. Each tube was sealed with Parafilm® before the cap was screwed on tightly to avoid any leakage and placed on a rotating axis (54 rpm) that is submerged in a water bath. The temperature of the water bath was set at 37 ± 2°C and maintained throughout the 24 h period of rotation to allow complete dissolution of the compounds. To eliminate all remaining solid particles, the solutions were individually filtered through 0.45 $\mu$m Millipore® filters into vials. A validated high performance liquid chromatography (HPLC) method was used to determine the concentration of the AZM in each solution (15).

**Dissolution**

Dissolution testing of AZM-DH and AZM-A were done in buffered media (pH 4.5, 6.8, 7.2) and deionised water. A VanKel700 dissolution bath was used for the dissolution testing. USP apparatus 2 (paddle) was set up at 37 ± 2°C with a rotational speed of 100 rpm, 900 mL of either pH 4.5, 6.8, 7.2 buffered media or deionised water was added to each dissolution vessel. Approximately 600 mg AZM and 300 mg glass beads, >106 µm (Sigma Aldrich, South Africa) were weighed into test tubes. 5 mL of dissolution medium of which the temperature was maintained at 37°C was pipetted into each test tube. The mixtures were then agitated for a period of 120 seconds, using a vortex mixer. The resulting mixtures were added to each dissolution vessel, 2 minutes apart. Samples of 5 mL were withdrawn from each dissolution vessel at predetermined time intervals. After withdrawal, the samples were filtered through a 0.45 µm PVDF filter into an HPLC vial. The filtered solutions were analysed by HPLC (15).

## *In vitro* permeability of different azithromycin forms

### Preparation of solutions for permeability study

The *in vitro* transport of AZM-DH and AZM-A was determined in three different transport media, which included Krebs Ringer bicarbonate buffer at pH 7.2, Krebs Ringer bicarbonate buffer adjusted to pH 6.8 and Krebs Ringer bicarbonate buffer adjusted to pH 4.5. In order to establish the effect of solubility on the membrane permeability of the two AZM forms, oversaturated solutions were prepared in each of the transport media. A concentration of 2 mg/mL was used to ensure a saturated solution for the transport studies in Krebs Ringer bicarbonate buffer at pH 7.2 and pH 6.8 and a concentration of 9 mg/mL was used to ensure a saturated solution for the transport study in Krebs Ringer bicarbonate buffer at pH 4.5. The dispersions were ultrasonicated for 5 minutes prior to commencement of the transport study.

### Preparation of tissue

A small piece (approximately 30 cm) of intestinal tissue was collected at the local abattoir from freshly slaughtered pigs and carefully washed with cold Krebs Ringer bicarbonate buffer. The small intestinal tissue was then placed in a container filled with cold Krebs Ringer bicarbonate buffer to be transported. Preparation of the tissue for the transport study was done within 1 h after collection of the tissue at the abattoir. On arrival at the laboratory, the acquired piece of small intestine was washed with cold Krebs Ringer bicarbonate buffer, where after it was carefully hauled over a glass tube. The serosal layer of the small intestinal tissue was cautiously removed by making a superficial incision along the mesenteric border and then slowly pulling the whole serosal layer off as it separates from the mucosal layer. The tissue remaining on the glass tube was then thoroughly inspected for weaknesses or thickened areas (e.g. Payer's patches) that may negatively influence the transport results of the study. After this, the mesenteric border was used as guideline to dissect the intestinal tube open to produce a flat

sheet of tissue. The dissected tissue was then rinsed with cold Krebs Ringer bicarbonate buffer to remove it from the glass tube onto a strip of filtration paper. The tissue was then cut into small pieces (approximately 3 cm in width) and mounted between two half cells (Ussing-type chamber) of a Sweetana-Grass diffusion apparatus. The surface area of the mucosal tissue that was exposed for transport is 1.78 $cm^2$. The six diffusion chambers were placed in the diffusion apparatus and coupled to a heating block maintained at a temperature of 37˚C (9,16).

Pre-heated (37˚C) Krebs Ringer bicarbonate buffer (7 mL) was placed at both sides (apical and basolateral) of the tissue whilst medical oxygen was constantly bubbled through the chambers for 30 minutes to allow the tissue to adapt to the environment. The buffer was then removed from the chambers and the basolateral sides were refilled with 7 mL of fresh Krebs Ringer bicarbonate buffer (also 37˚C). After filling the apical sides with 7 mL of test compound solution, the trans-epithelial electrical resistance (TEER) was measured with a Millicell® ERS-2 epithelial volt/ohm meter. These measurements were performed again at the end of the study prior to the last withdrawals as an indication of the integrity of the excised intestinal tissue (9).

The volume of each sample was 200 µL, which were withdrawn from the basolateral chambers at 20, 40, 60, 80, 100, and 120 minutes after application of the test solutions in the apical chambers. Each sample that was withdrawn was immediately replaced with 200 µL Krebs Ringer bicarbonate buffer (37˚C). The samples were analysed by means of HPLC to determine the concentration of AZM.

**Data analysis**

Data obtained from the HPLC analyses were processed to determine the amount of AZM-DH and AZM-A that permeated across the excised pig intestinal tissue over time. The cumulative percentage AZM transported was plotted as a function of time and the apparent permeability coefficient ($P_{app}$) values were calculated for each transport experiment. The $P_{app}$ value in this

study represents the normalised amount of AZM transported across the exposed tissue surface area from the apical side of the diffusion chamber. The $P_{app}$ values were calculated with the following equation (17):

$$P_{app} = (dC/dt) \times (1/A \bullet C_0 \bullet 60) \quad (1)$$

where $dC/dt$ represents the rate of transport (slope of % transport vs time curves); A is the surface area (1.78 $cm^2$) of the intestinal tissue; and $C_0$ accounts for the initial AZM concentration (µg/mL). Statistical analysis (ANOVA, single factor using MS Office Excel® software) was performed to determine if differences in the transport were statistically significantly ($p \leq 0.05$) between the two AZM forms at each pH value.

## Results

### Physico-chemical characterization of azithromycin solid-state forms

The FTIR spectrum of AZM-DH (Figure 2a) displays characteristic sharp peaks at 3567, 3496 and 3236 $cm^{-1}$, these peaks represent free hydroxyl, hydrogen bonded hydroxyl and intramolecular hydrogen bonded hydroxyl functional groups, respectively (18-20). In contrast to AZM-DH, the amorphous AZM-A (Figure 2b) shows only a broad absorption peak at 3500 $cm^{-1}$, which corresponds to a hydroxyl group stretch. The peak broadening is attributed to the random arrangement of the azithromycin molecules as it exists in an amorphous phase. This random arrangement of molecules will also result in a hydrogen bonding state that will differ from one molecule to the other. Furthermore, the IR spectrum of AZM-A correlates well with the fact that peak broadening occurs with amorphous forms when compared to crystalline forms (21-22).

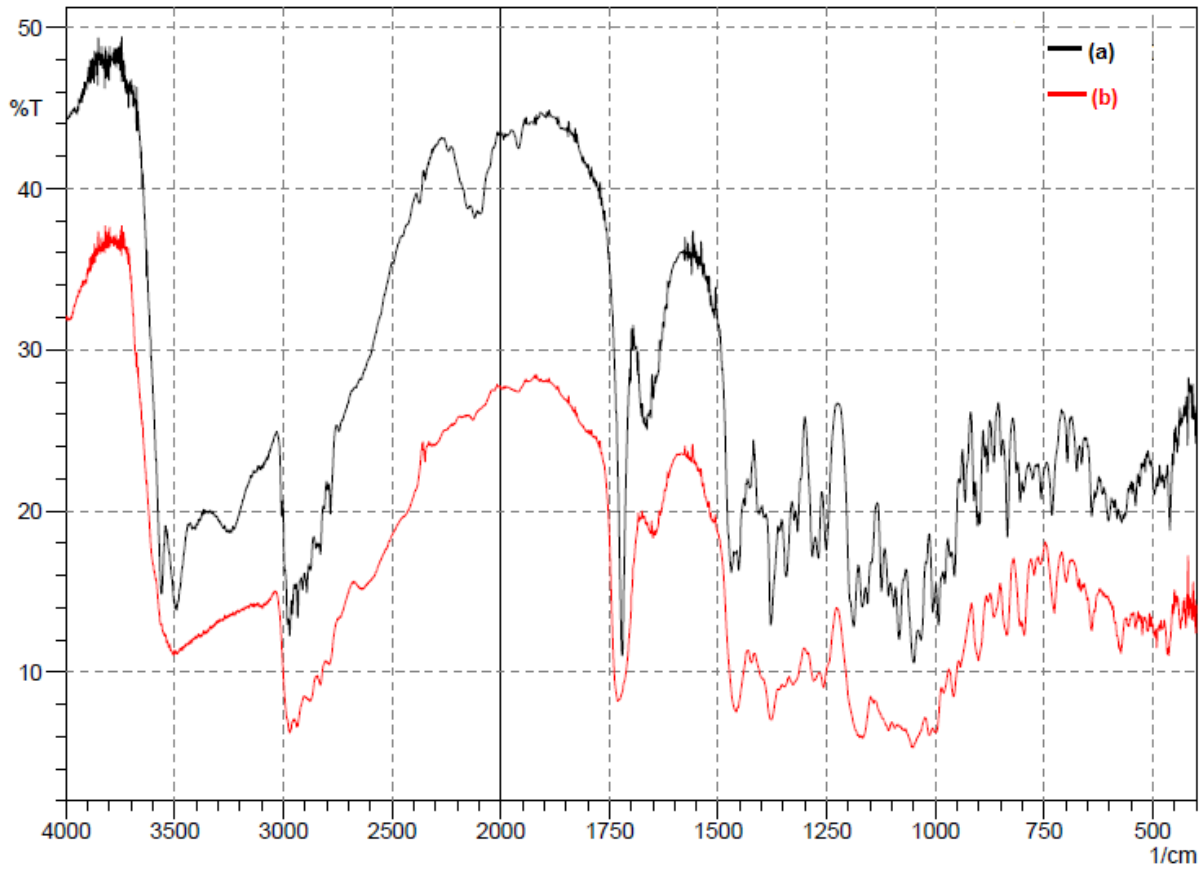


**Figure 2:** FTIR spectra of (a) AZM-DH and (b) AZM-A.

The XRPD patterns of AZM-DH and AZM-A (Figure 3a and b) confirmed the amorphous habit of quench cooled AZM. Figure 3a illustrates characteristic peaks of a crystalline material, which are detected at various scattering angles (˚2$\theta$) with variable intensities. The XRPD pattern of the AZM-A sample showed no characteristic peaks (Figure 3b); only a typical amorphous halo pattern. The absence of peaks on the XRPD pattern of AZM-A means that there is no long-range order of molecular packing like the crystalline form and therefore AZM-A can be regarded as amorphous.

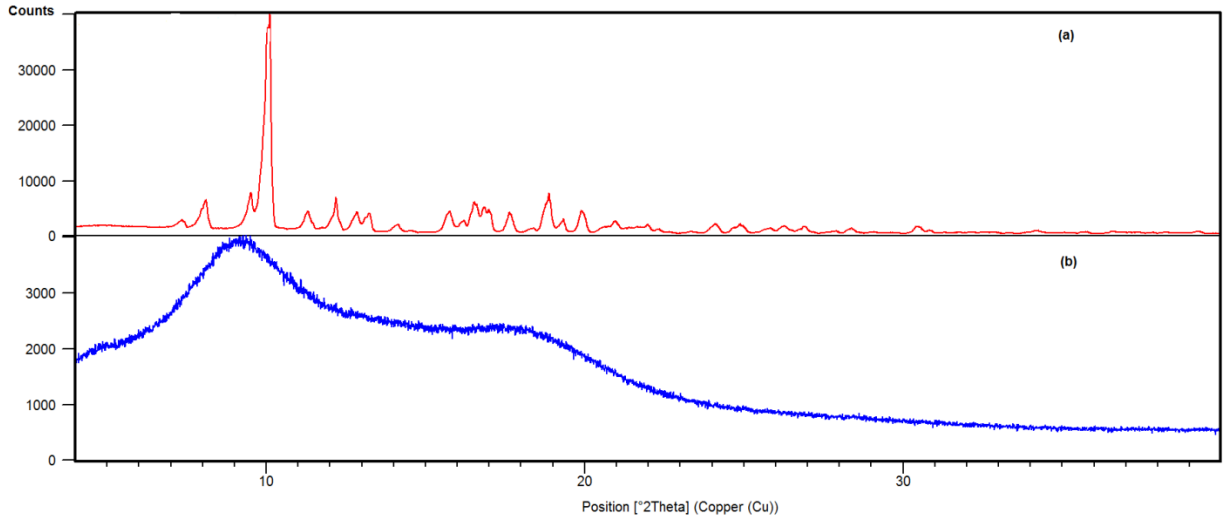


**Figure 3:** Overlay of the XRPD patterns obtained for (a) AZM-DH and (b) AZM-A.

The DSC thermogram of AZM-DH illustrated two dehydration endotherms (76.35˚C and 86.45˚C) of the dihydrate, followed by the subsequent melting event at 119.04˚C (Figure 4a). In contrast to the thermogram of AZM-DH (Figure 4b), no dehydration endotherms were visible for AZM-A, but displayed only a glass transition at 106.65˚C.

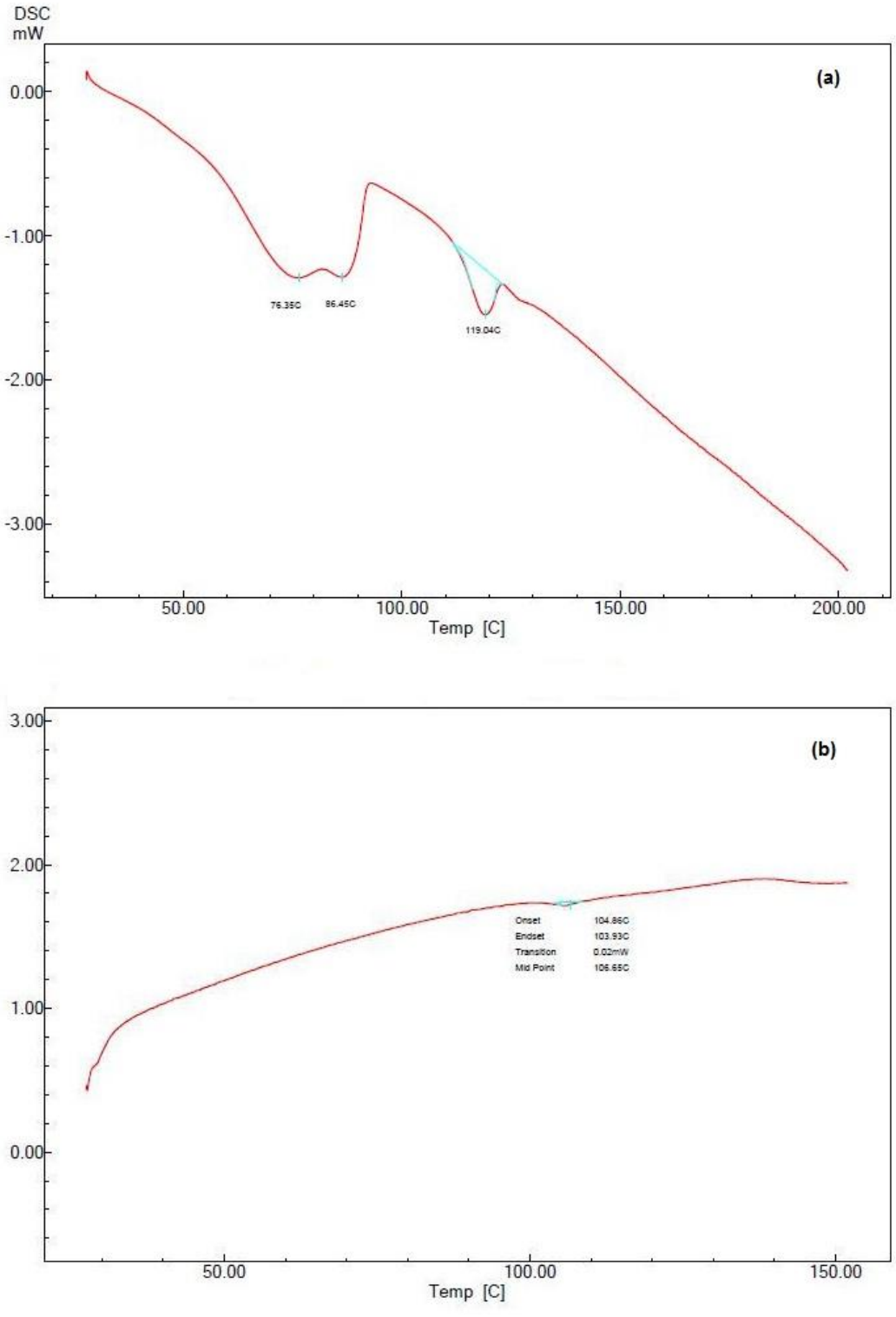


**Figure 4:** DSC thermograms of (a) AZM-DH and (b) AZM-A.

TG analysis of AZM-DH exhibited a 4.40% weight loss compared to the initial weight of the AZM-DH sample, which can be attributed to the loss of water molecules upon dehydration. This correlates well with the calculated theoretical weight loss of 4.59% (5). The TGA thermogram of AZM-A showed a weight loss of only 0.61%, which is markedly less than the percentage weight loss of a monohydrate (i.e. 2.30%) (5). According to the Karl Fischer titration, AZM-DH contained 4.59% water, which is exactly the same as the theoretical water content of the dihydrate. The water content for AZM-A determined by Karl Fischer titration was 0.61%, which confirms the results obtained with TGA.

**The effect of water on amorphous azithromycin**

Vapor sorption results of both AZM-DH and AZM-A are shown in Figures 5 and 6. The sorption data obtained for AZM-DH showed an insignificant increase (1.2%) in percentage weight up to a relative humidity of 95%. Although the sorption isotherm started at 0%RH, the drying conditions (50˚C for 60 minutes) proved to be insufficient to dehydrate AZM-DH to the monohydrate or the anhydrate. This increase in moisture can therefore be ascribed to condensed moisture on the surface of the powder and the sample container, rather than hydration of the sample. The isotherms showed little to no hysteresis, therefore indicating that the decline in sample moisture occurred at approximately the same rate as during the adsorption phase. XRPD analysis confirmed the fact that AZM-DH remained in the dihydrated form during the vapor sorption experiments, since the resulting diffractogram compared well with the diffractogram presented in Figure 3(a).

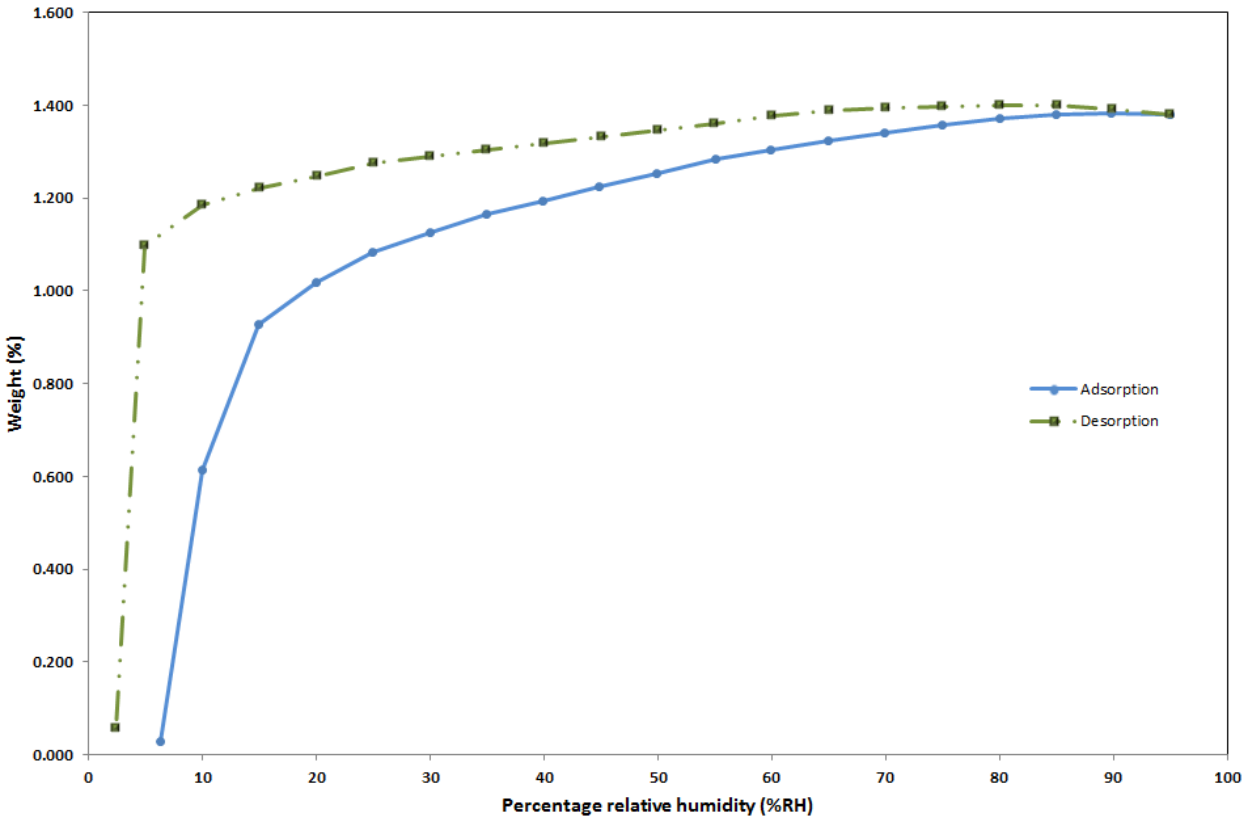


**Figure 5:** Vapor sorption data obtained for AZM-DH.

Figure 6 depicts the vapor sorption isotherms obtained for AZM-A. According to the isotherm AZM-A showed an increase in sample weight of 1.0% up to a relative humidity of 50% RH, followed by a rapid increase in the sample weight up to 5.0% from 60 – 90% RH.

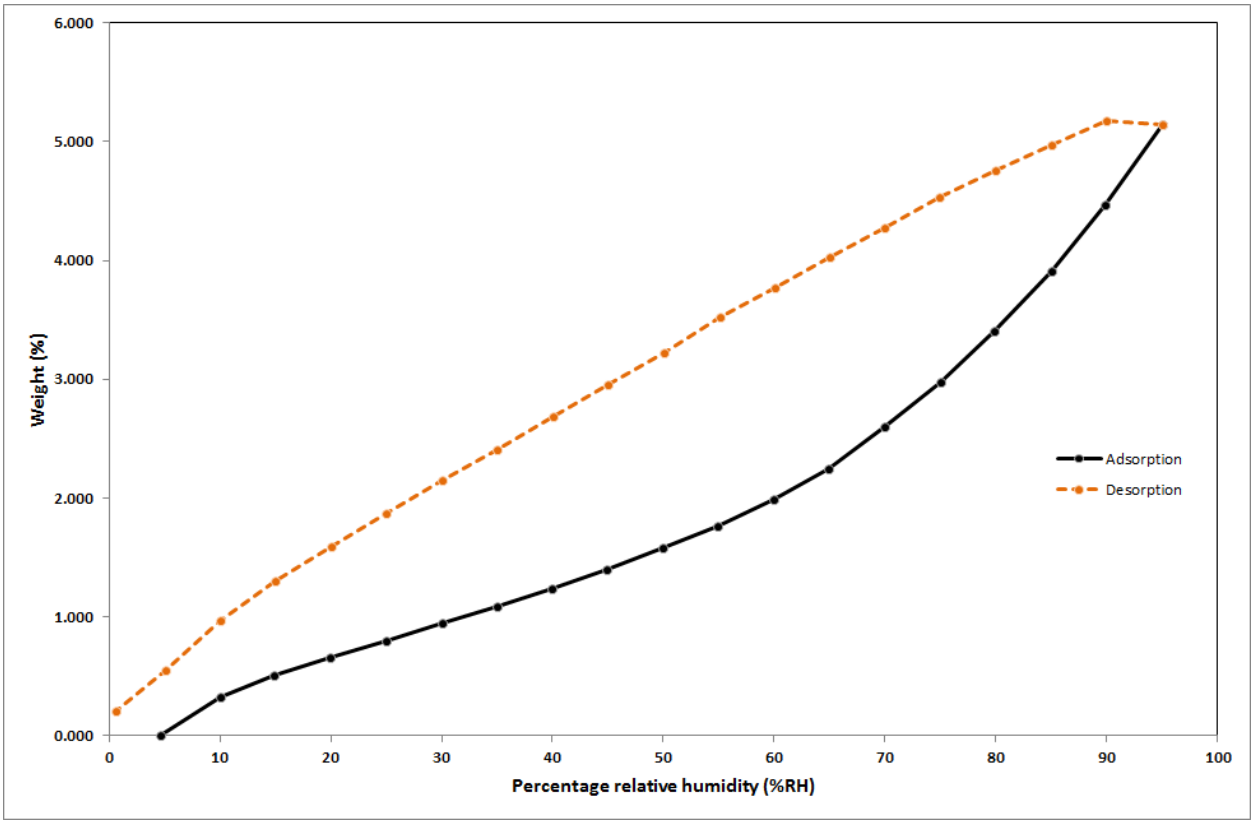


**Figure 6:** Vapor sorption data obtained for AZM-A.

However, during the subsequent desorption (90% - 0% RH) phase a weight loss of 5.0% was observed, returning to the initial weight. It should be mentioned that this isotherm shows hysteresis. Since the most common cause for hysteresis is the condensation of water in pores or capillaries during the adsorption phase (23), it was decided to look into the morphological differences between AZM-DH and AZM-A. Figure 7 shows SEM-images obtained for both AZM-DH and AZM-A.

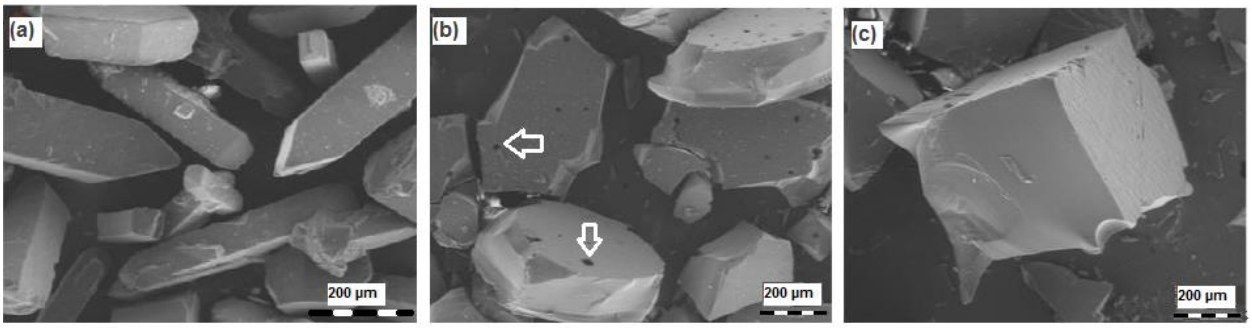


**Figure 7:** SEM images of (a) AZM-DH, (b) AZM-A with white arrows indicating cavities and (c) AZM-A.

From the SEM-images small cavities on the surface of AZM-A (Figure 7(b)) can be observed. These cavities are probably due to air bubbles being trapped during the quench cooling process. Therefore, it is possible that during vapor sorption experiments, moisture condense in these cavities, resulting in a slower rate of desorption of moisture, which is subsequently observed as hysteresis on the moisture sorption isotherm. It is therefore evident that vapor sorption does not induce recrystallization of AZM-A to AZM-DH.

**Equilibrium solubility in different media**

The resulting concentrations from the solubility determination of AZM-DH and AZM-A in the different media are listed in Table 1. The solubility results indicated that AZM-A shows mentionable higher solubility concentrations in comparison with AZM-DH in Krebs Ringer buffers with pH values of 6.8 and 7.2, but not in the buffer at pH 4.5. The increase in solubility concentration of AZM-A compared to that of AZM-DH was most prominent in deionised water. Statistically the difference in solubility concentrations of AZM-DH and AZM-A in either pH 6.8, 7.2 and deionised water proved to be extremely significant, with $p<0.0001$. While, solubility concentrations of AZM-DH and AZM-A in pH 4.5 proved to be not statistically different ($p> 0.05$). Since AZM is a basic drug, it becomes more ionized the further the pH drops below its $pK_a$ value

of 8.74, which explains why AZM-DH and AZM-A show similar solubility concentrations at the relatively low pH value of 4.5.

**Table 1:** Concentrations of AZM-DH and AZM-G achieved in the different transport media

| | **AZM-DH (µg/mL)** | **AZM-A (µg/mL)** |
|---|---|---|
| **Krebs Ringer bicarbonate buffer (pH 7.2)** | 480 | 710 |
| **Krebs Ringer bicarbonate buffer (pH 6.8)** | 1240 | 1500 |
| **Krebs Ringer bicarbonate buffer (pH 4.5)** | 8600 | 8400 |
| **Distilled Water** | 70 | 300 |

**Dissolution**

The powder dissolution profiles for AZM-DH and AZM-A in buffered media (pH 4.5, 6.8. 7.2) as well as in deionised water are presented in Figures 8-11. Concentrations of higher than 85% of both AZM-DH and AZM-A were already achieved after 5 minutes in all the buffered media (Figure 8-10).

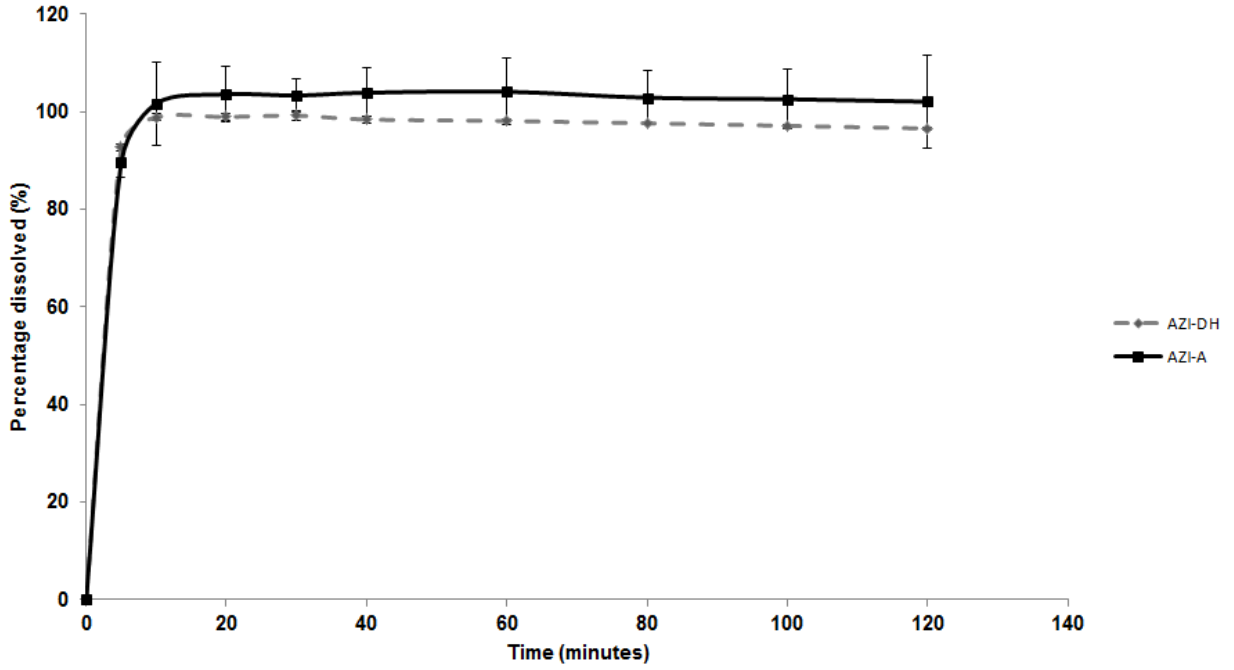


**Figure 8:** Dissolution profiles of AZI-DH and AZI-A in pH 4.5 buffered medium.

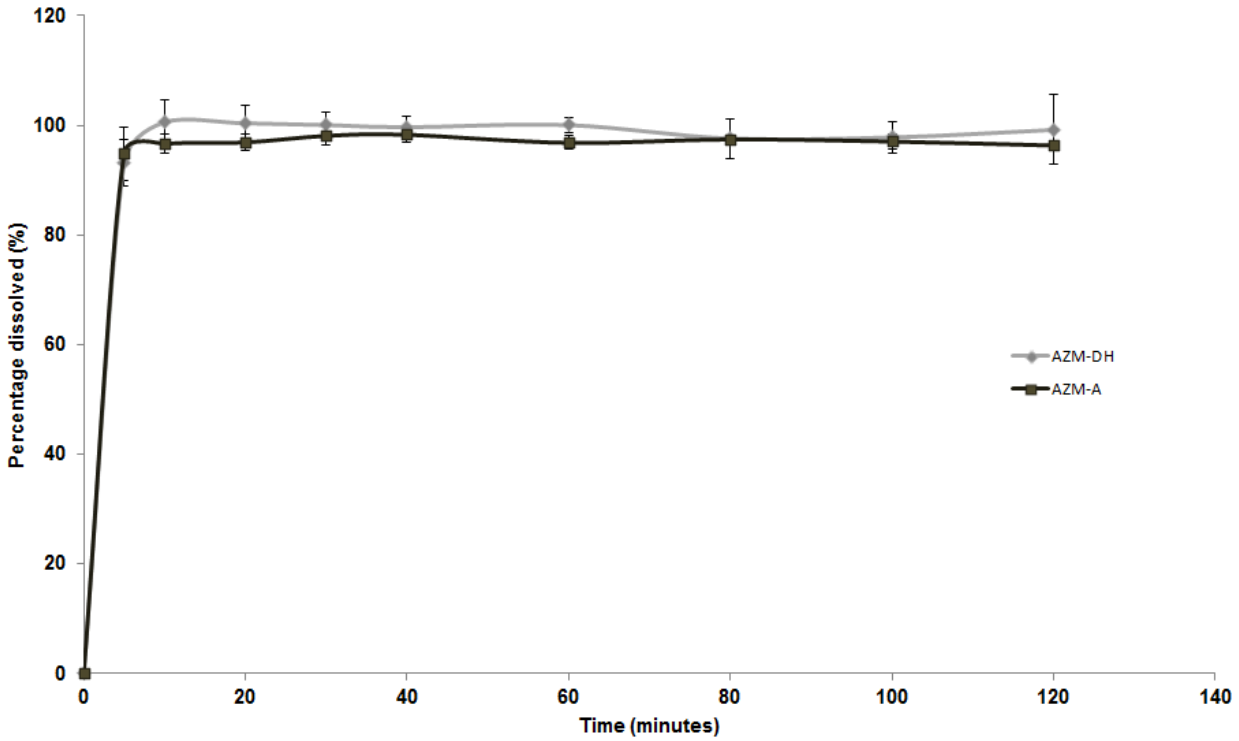


**Figure 9:** Dissolution profiles of AZM-DH and AZM-A powder in pH 6.8 buffered medium.

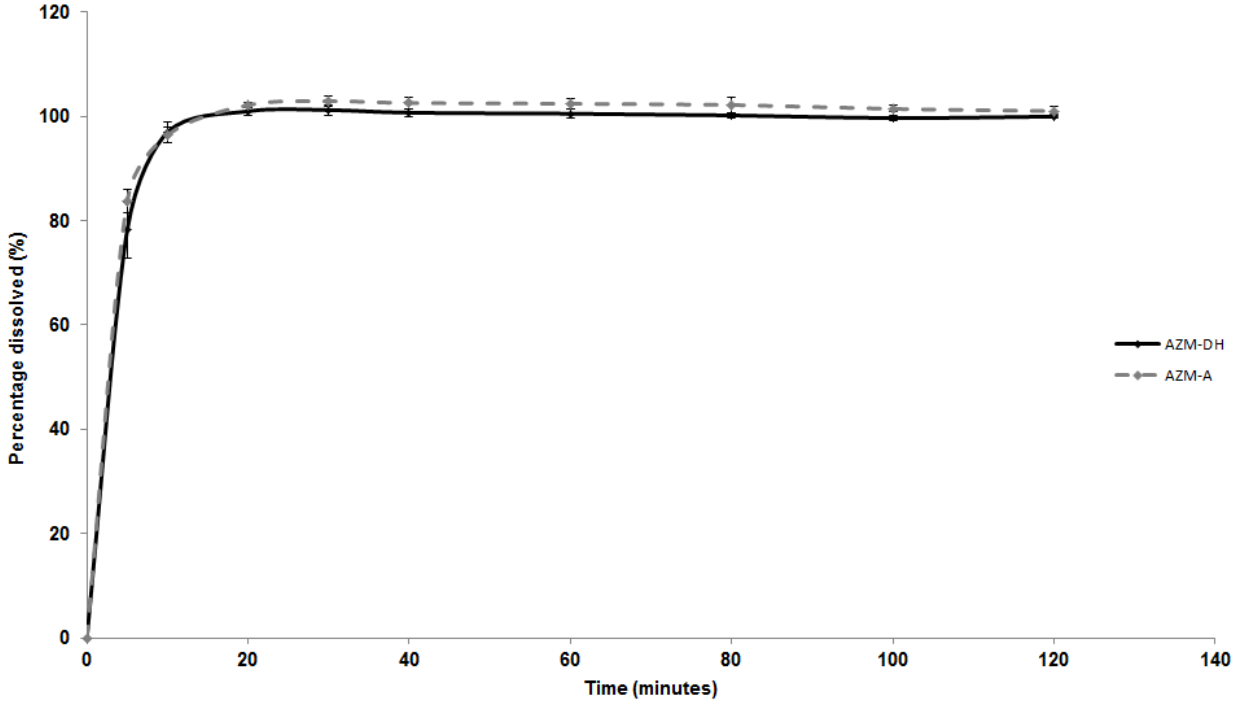


**Figure 10:** Dissolution profiles of AZM-DH and AZM-A in pH 7.2 buffered medium.

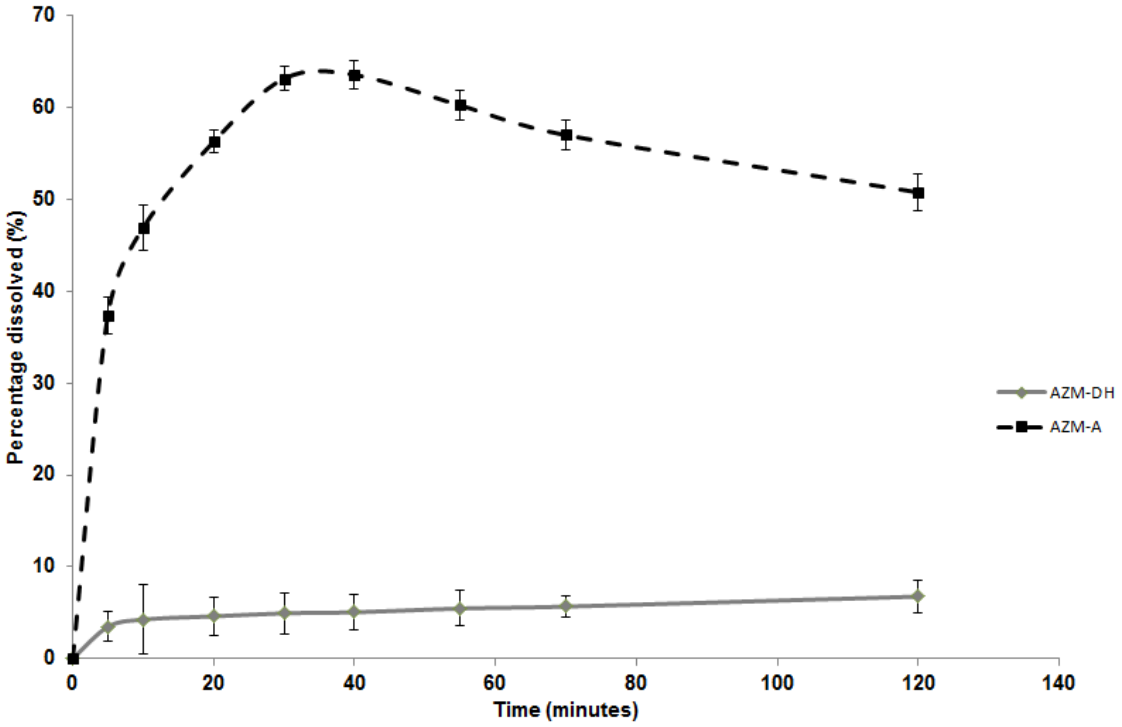


**Figure 11:** Dissolution profiles of AZM-DH and AZM-A powder in distilled water.

The dissolution in distilled water resulted in statistically significant differences ($p < 0.05$) in the percentage AZM dissolved (Figure 11) over the entire period of the dissolution test. The rate of dissolution for AZM-A was much higher than that of AZM-DH. Amorphous forms have higher aqueous solubility than the crystalline forms of the same active compound due to the fact that for an amorphous solid less energy is required to transfer one molecule to the solvent/solution. Taking this into consideration, it is expected that AZM-DH should have a lower dissolution rate and dissolved concentration than AZM-A. The decrease in the percentage dissolved (%) can be attributed to solution-mediated phase transformation. This transformation is associated with the precipitation of a stable, less soluble form of a given API during the dissolution of a metastable form (24). In this study the possibility of such a transformation resulted in a 12.8% (0.06 mg/mL) decrease in the dissolved concentration. We consider this decrease in the dissolved concentration to have a negligible effect on the permeability studies. The reason for proposing this are explained by the data reported by previous studies (24,25) which discussed the importance of supersaturated solutions in order to induce solution-mediated phase transformation. These studies showed that continuous dissolution media replacement prevents solution-mediated phase transformation.

***In vitro* transport study**

The apparent permeability coefficient ($P_{app}$) values for AZM-DH and AZM-A obtained in Krebs Ringer Bicarbonate buffer with three different pH values are shown in Table 2. The p-values obtained from the ANOVA analysis of the $P_{app}$ values for AZM-DH and AZM-A at each pH value is also included in Table 2.

**Table 2** Results of the statistical analyses for AZM-DH and AZM-G in various media at different pH values.

| | pH 7.2 | | pH 6.8 | | pH 4.5 | |
|---|---|---|---|---|---|---|
| | **AZM-DH** | **AZM-G** | **AZM-DH** | **AZM-G** | **AZM-DH** | **AZM-G** |
| **Replicates** | 6 | 6 | 6 | 6 | 6 | 6 |
| **Avg. $P_{app}$ ($x10^{-6}$ cm/s)** | 0.000 | 2.680 | 1.960 | 3.300 | 0.874 | 0.367 |
| **p-value** | $1.67 \times 10^{-12}$ | | $9.00 \times 10^{-8}$ | | $3.47 \times 10^{-4}$ | |

When Krebs Ringer Bicarbonate buffer with a pH of 4.5 was used as the transport medium, the concentration of AZM-DH in the basolateral chamber after 120 minutes was 95.2 µg/mL. This constitutes a total cumulative percentage transport of 1.1% of the initial AZM-DH dose applied to the apical chamber. The concentration of AZM-A in the basolateral chamber after 120 minutes was 44.6 µg/mL, which relates to a total cumulative percentage transport of 0.5% of the initial AZM-A dose applied. The calculated $P_{app}$ values for AZM-DH and AZM-A were 0.874 x $10^{-6}$ cm/s and 0.367 x $10^{-6}$ cm/s respectively (Figure 12), which are statistically significantly different ($p < 0.05$). The transport of the two AZM forms across excised pig intestinal tissue corresponded with their solubilities in buffer with a pH of 4.5. Since saturated solutions were used in the permeability studies, AZM-A was less soluble than AZM-DH at pH 4.5 and therefore a lower concentration gradient existed for AZM-A across the excised pig intestinal tissue compared to that of AZM-DH, which resulted in a lower transport rate and extent.

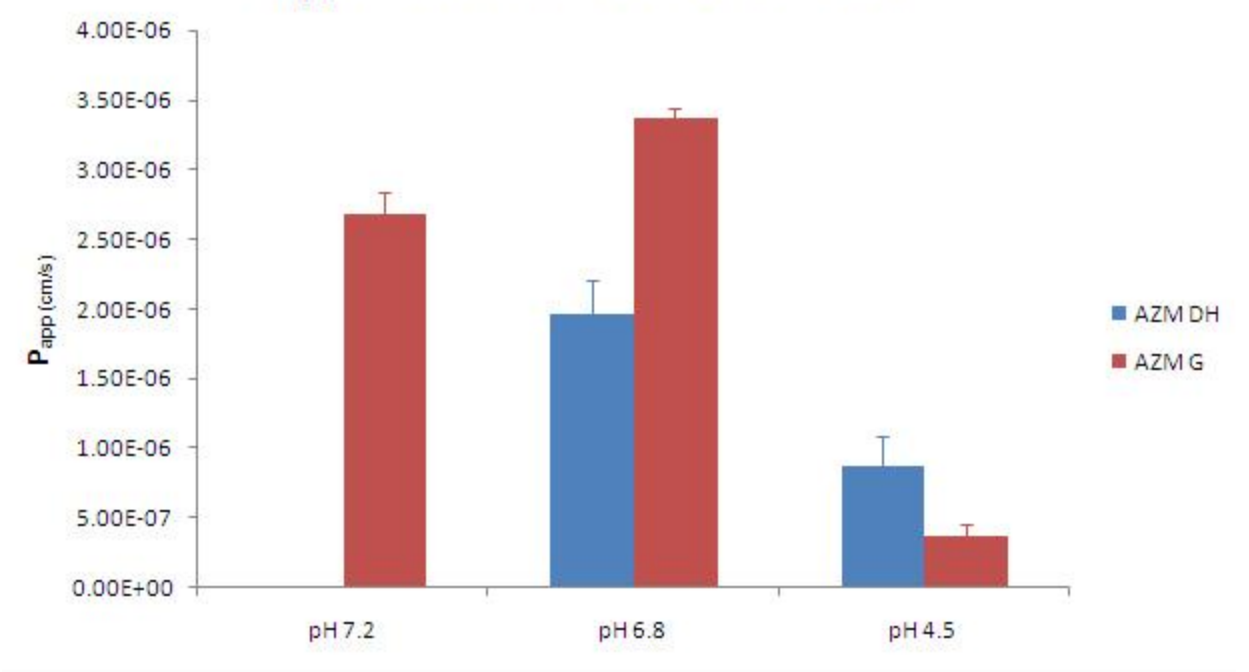


**Figure 12:** Results of the Papp values achieved for AZM-DH and AZM-G in various buffered media.

A total cumulative percentage transport of 2.6% was achieved for AZM-DH and 5.0% for AZM-A in Krebs Ringer Bicarbonate buffer with a pH of 6.8 across the excised pig intestinal tissue over a period of 120 min. The calculated average $P_{app}$ values for AZM-DH and AZM-A were 1.96 x $10^{-6}$ cm/s and 3.37 x $10^{-6}$ cm/s respectively (Figure 12), which are statistically significantly different ($p < 0.05$). In Krebs Ringer Bicarbonate buffer with a pH of 7.2, the final concentration of AZM-A at the basolateral side after 120 minutes was 51.2 µg/mL, while AZM-DH was not detectable over the entire period of the transport study. The cumulative percentage AZM-A that was transported from the apical to the basolateral side across the excised pig intestinal tissue constitutes 3.71% of the initial dose applied to the apical side and $P_{app}$ value of 2.68 × $10^{-6}$ cm/s. The significantly higher transport of AZM-A across excised pig intestinal tissue compared to that of AZM-DH at both pH 6.8 and 7.2 is in agreement with the increase in solubility of the

amorphous form (i.e. AZM-A) over the dihydrate crystalline form (i.e. AZM-DH) in saturated solutions at these pH values.

The physical change of crystalline AZM-DH to the amorphous form (AZM-A) not only improved the solubility of AZM but also improved its epithelial membrane permeability in a pH dependent way. The AZM-A form therefore provides the possibility to achieve the acquired plasma levels at lower doses compared to that of AZM-DH due to the increased solubility and permeability, however, it should be confirmed with *in vivo* studies before final conclusions can be drawn.

**Conclusion**

The amorphous form of azithromycin (AZM-A) prepared in this study exhibited a significantly higher water solubility and dissolution rate compared to the commercially available azithromycin dihydrate (AZM-DH) raw material. AZM-A was also significantly more soluble than AZM-DH in buffers with pH values of 6.8 and 7.2, but did not show a statistical difference in pH 4.5 buffered media. Dissolution studies confirmed the solubility results and also showed the significant improvement in water solubility of AZM-A in comparison with AZM-DH. Although solution-mediated phase transformation of AZM-A to AZM-DH was identified during the dissolution studies it proved to have a negligible effect on the permeability determinations. The permeability of AZM-A across excised pig intestinal tissue correlated well with its increased solubility compared to that of AZM-DH at pH values of 6.8 and 7.2 probably due to an increased concentration gradient. The improved water solubility together with the increased epithelial membrane permeability provides the potential to obtain increased oral bioavailability with AZM-A compared to that of AZM-DH.

**References**

1. Nakornchai, S and Konthiang, P. Activity of azithromycin or erythromycin in combination with antimalarial drugs against mulitdrug-resistant *Plasmodium falciparum in vitro*. Acta Tropica. 2006;100:185-191.

2. Ferrara A, Dos Santos C, Cimbro M, Gialdroni Grassi G. Comparative antimicrobial activity and post-antibiotic effect of azithormycin, clarithromycin and roxithromycin against some respiratory pathogens. Int. J. Antimicrob. Agents. 1996;7:181-186.

3. Boonleang J, Panrat K, Tantana C, Krittathanmakul S, Jintapakorn W. Bioavailability and pharmacokinetic comparison between generic and branded azithromycin capsule: A randomised, double blind, 2-way cross-over in healthy male Thai volunteers. Clin Ther 2007;29:703-710.

4. Montejo-Bernardo J, Garcia-Granda S, Bayod-Jasanada M, Llorente I, Llavona L. An easy and general method for quantifying Azithormycin dihydrate in a matrix of amorphous Azithromycin. ARKIVOC. 2005; (ix) 321-331.

5. United States Pharmacopoeia. National Formulary 30, The United States Pharmacopoeial Convention, 2013; 35$^{th}$ edition NF.

6. Arora S.C, Sharma P.K, Irchhaiya R, Khatkar A, Singh N, Gagoria J. Development , characterization and solubility of solid dispersions of azithromycin dihydrate by solvent evaporation method. J Adv Pharm Technol Res. 2010;1(2):221-228.

7. Yu L. Amorphous pharmaceutical solids: preparation, characterization and stabilization. Adv Drug Deliv Rev. 2007;48:27-42.

8. Ashford M. Assessment of biopharmaceutical properties. In Aulton ME, editor. Pharmaceutics. The science of dosage form design, New York: Churchill Livingstone, 2002. p. 259.

9. Berggren S, Hoogstraate J, Fagerholm U, Lennernäs, H. Characterization of jejunal absorption and apical efflux of ropivacaine, lidocaine and bupivacaine in the rat using *in situ* and *in vitro* absorption models. Eur J Pharm Sci. 2004;21:553-560.

10. Balimane P.V, Chong S, Morrison R.A. Current methodologies used for evaluation of intestinal permeability and absorption. J Pharmacol Toxicol Methods. 2000;44:301-312.

11. Hunter J, Hirst B.H. Intestinal secretion of drugs. The role of P-glycoprotein and related drug efflux systems in limiting oral drug absorption. Adv Drug Deliv Rev. 1997;25:129-157.

12. Kerns E.H, Di L. Drug-like properties, concepts, structure design and methods: from ADME to toxicity optimization, San Diego: Academic Press. 2008;p. 526.

13. Nožinić D, Milić A, Mikac L, Ralić J, Padovan J. Antolović R. Assessment of macrolide transport using PAMPA, Caco-2 and MDCKII-hMDR1 assays. Croat Chem Acta. 2010;83: 323-331.

14. Neirinckx E, Vervaet C, Michiels J, De Smet S, Van Den Broeck W, Remon JP, De Backer P, Croubels S. Feasibility of the Ussing chamber technique for the determination of *in vitro* jejunal permeability of passively absorbed compounds in different animal species. J Vet Pharmacol Ther. 2010;34, 290–297.

15. Odendaal RW, Aucamp ME, Liebenberg W.. A novel reversed-phase LC method for quantitative detection of azithromycin in bulk drug and tablet formulations in various aqueous media. Pharmazie, 2012;67, 984 - 986.

16. Tukker JJ. *In vitro* methods for the assessment of permeability. In Dressman JB, Lennernäs H, editors. Oral drug absorption, prediction and assessment. New York: Marcel Dekker Inc. 2000;p. 51-72.

17. Hansen TS, Nilsen OG. *Echinacea purpurea* and P-Glycoprotein drug transport in Caco-2 cells. Phytother Res. 2009;23:86-91.

18. Brittain H.G. Methods for the characterization of polymorphs and solvates. In Brittain HG, editor. Polymorphism in pharmaceutical solids, New York: Marcel Dekker Inc. 1999; p. 227-278.

19. West AR. 1999. Basic solid state chemistry. 2nd ed. New York: Wiley & Sons, LTD. 1999; p. 480.

20. Gandhi R, Pillai O, Thilagavathi R, Gopalakrishnan B, Kaul CL, Panchagnula R. Characterization of azithromycin hydrates. Eur J Pharm Sci 2002;16:175-184.

21. Yu L, Reutzel SM, Stephenson GA. Physical characterization of polymorphic drugs: an integrated characterization strategy. Pharm Sci Technol Today 1998; 1:118-127.

22. Chieng N., Rades T, Aaltonen J. An overview of recent studies on the analysis of pharmaceutical polymorphs. J Pharm Biomed Anal 2011; 55:618-644.

23. Wolf M, Walker JE, Kapsalis JG. Water vapor sorption hysteresis in dehydrated food. J Agr Food Chem. 1972;20(5):1073-7.

24. Greco K, Bogner R. Solution-mediated phase transformation: Significance during dissolution and implications for bioavailability. J. Pharm Sci. 2012;101(9):2996-3018.

25. Aucamp M, Stieger N, Barnard N, Liebenberg W. Solution-mediated phase transformation of different roxithromycin solid-state forms: implications on dissolution and solubility. Int. J Pharm. 2013. doi:10.1016/j.ijpharm.2013.03.048.